

Supplementary Data

Co-produced natural ketolides methymycin and pikromycin inhibit bacterial growth by preventing synthesis of a limited number of proteins

Mashal M. Almutairi, Maxim S. Svetlov, Douglas A. Hansen, Nelli F. Khabibullina, Dorota Klepacki, Han-Young Kang, David H. Sherman, Nora Vázquez-Laslop, Yury S. Polikanov, Alexander S. Mankin

Content:

Supplementary Tables S1 and S2

Supplementary Figures S1 – S3

Table S1. X-ray data collection and refinement statistics.

<i>Crystals</i>	70S-MTM with A-, P- and E-tRNAs	70S-PKM with A-, P- and E-tRNAs
<i>Diffraction data</i>		
Space Group	P2 ₁ 2 ₁ 2 ₁	P2 ₁ 2 ₁ 2 ₁
Unit Cell Dimensions, Å (a x b x c)	209.62 x 448.78 x 622.53	209.34 x 447.21 x 620.61
Wavelength, Å	0.9795	0.9795
Resolution range (outer shell), Å	311-2.70 (2.77-2.70)	200-2.60 (2.67-2.60)
I/σI (outer shell with I/σI=1)	8.22 (1.06)	8.58 (0.97)
Resolution at which I/σI=1, Å	2.70	2.60
Resolution at which I/σI=2, Å	2.87	2.82
CC(1/2) at which I/σI=1, %	21.8	17.3
CC(1/2) at which I/σI=2, %	45.0	43.3
Completeness (outer shell), %	98.9 (95.0)	98.3 (96.4)
R _{merge} (outer shell)%	14.2 (118.5)	13.9 (122.1)
No. of crystals used	1	1
No. of Reflections Observed	5,320,880	5,786,516
Used: Unique	1,561,494	1,729,501
Redundancy (outer shell)	3.41 (3.39)	3.35 (3.19)
Wilson B-factor, Å ²	52.2	49.2
<i>Refinement</i>		
R _{work} /R _{free} , %	22.2/26.4	23.8/28.3
<i>No. of Non-Hydrogen Atoms</i>		
RNA	200,225	200,247
Protein	90,976	90,982
Ions (Mg, K, Zn, Fe)	2,879	2,423
Waters	5,102	3,394
<i>Ramachandran Plot</i>		
Favored regions, %	94.04	93.93
Allowed regions, %	5.18	5.30
Outliers, %	0.78	0.77
<i>Deviations from ideal values (RMSD)</i>		
Bond, Å	0.004	0.004
Angle, degrees	0.822	0.838
Chirality	0.040	0.040
Planarity	0.005	0.005
Dihedral, degrees	14.533	14.530
Average B-factor (overall), Å ²	59.3	52.7

R_{merge} = $\sum |I - \langle I \rangle| / \sum I$, where I is the observed intensity and $\langle I \rangle$ is the average intensity from multiple measurements.
R_{work} = $\sum |F_{\text{obs}} - F_{\text{calc}}| / \sum F_{\text{obs}}$. For calculation of R_{free}, 5% of the truncated dataset was excluded from the refinement.

Table S2.
Minimal inhibitory concentrations ($\mu\text{g/ml}$) of antibiotics against *E. coli* strains

Strain	Mutation	MTM	PKM	ERY	SOL	CHL
SQ110DTC ^a	WT	16	32	2	ND	1
	G2057U	>256	>256	>256	ND	1
	A2058G	>256	>256	>256	ND	1
	A2059G	>256	>256	>256	ND	1
	C2611U	>256	>256	>256	ND	1
BWDK ^b	WT	4	4	ND	0.5	0.8

^a) MIC for SQ110DTC cells was determined in LB medium

^b) MIC for BWDK cells was determined in minimal M9 medium lacking methionine, but supplemented with the other 19 amino acids.

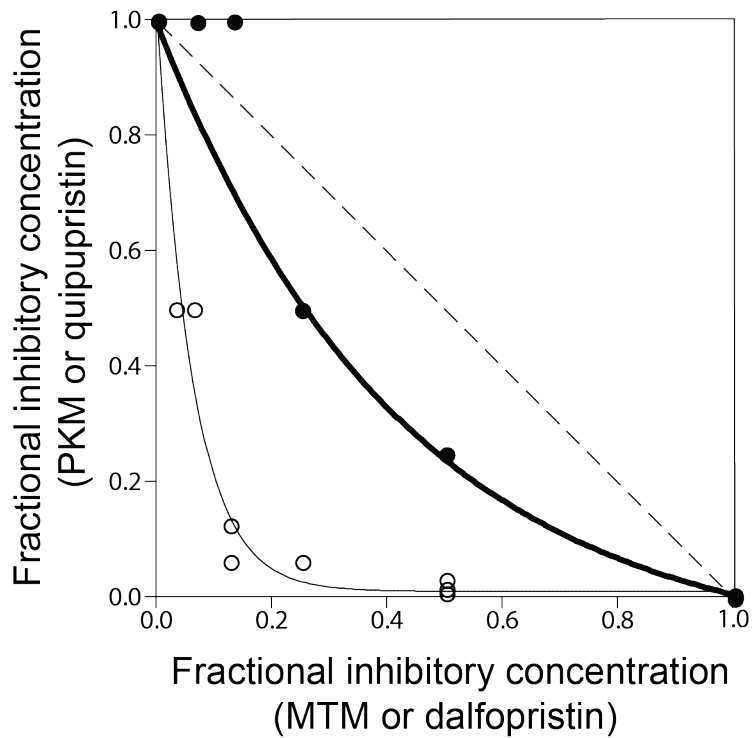


Figure S1. The checkerboard testing of possible synergy between MTM and PKM reveals them as essentially additive antibiotics. Black circles: the MTM/PKM combinations, open circles: the combinations of the ribosome-targeting synergistic streptogramin antibiotics quinupristin and dalfopristin. The dashed diagonal line approximates the fractional inhibitory concentrations (FIC) values for a hypothetical pair of ideally additive antibiotics.

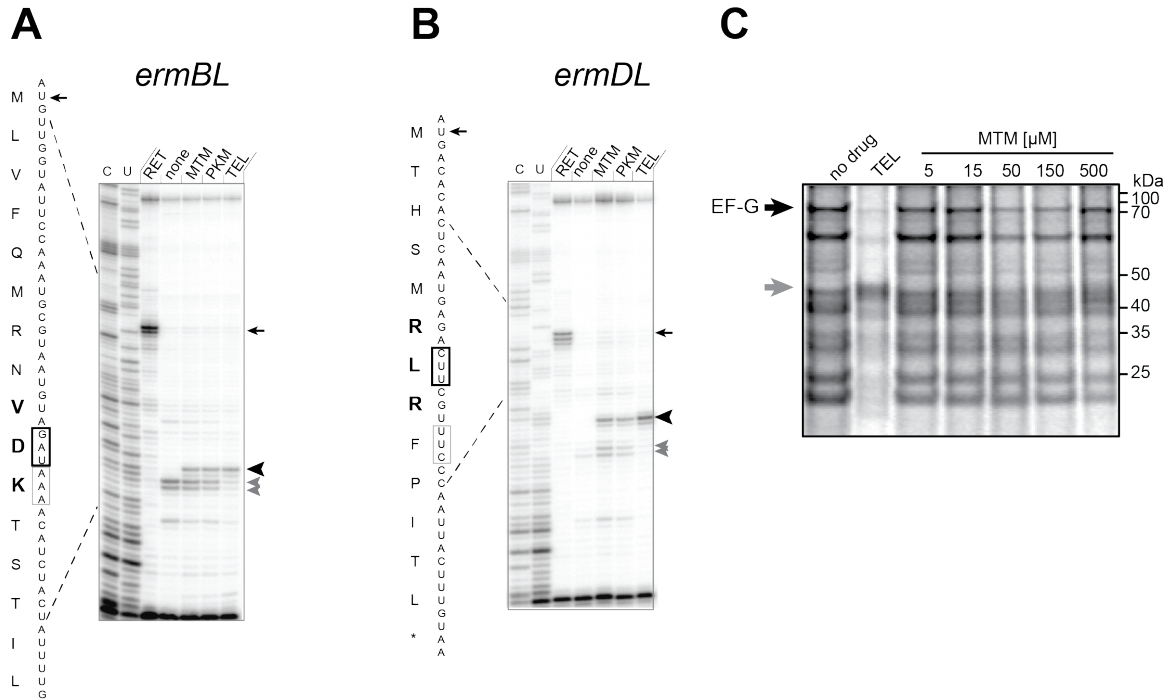


Figure S2. MTM and PKM inefficiently arrest translation at the motifs problematic for the ketolide-bound ribosome. (A) and (B): In vitro toeprinting analysis comparing the efficiency of ketolides TEL, MTM and PKM in causing ribosomal arrest at the VDK sequence of *ermBL* (A) or the RLR motif of *ermDL* (B). Positions of the toeprint bands (which are 16-17 nts downstream from the first nucleotide of the P-site codon) generated by ribosomes stalled due to the presence of MTM, PKM or TEL are indicated on the gels by black arrowheads. The codon in the P site of the ketolide-stalled ribosome is boxed in a black frame in the sequence of the corresponding genes. Ribosomes that escape ketolide-mediated stalling are captured at the Lys codon of *ermBL* (A) or the Phe codon of *ermDL* (B) (boxed in grey frames) because of the presence in the reactions of (A) Thr-RS inhibitor (borrelidine) or (B) Pro-RS inhibitor (L-PSA), respectively. The toeprint bands of the captured ribosomes are marked with grey arrowheads. The toeprint bands of the ribosomes arrested at the start codons of *ermBL* and *ermDL* because of the presence of the initiation inhibitor retapamulin (RET), are indicated by an arrow. The control sample labelled as “none” had no ketolides or retapamulin added, but contained the respective RS inhibitor. (C) In vitro translation in the *E. coli* S30 extract of the *fusA* gene encoding the 78 kDa protein EF-G. Translation reactions, supplemented with [³⁵S]-L-methionine, were carried out in the absence of antibiotics (‘no drug’), in the presence of 50 μM of TEL or in the presence of the indicated concentrations of MTM. The black arrow indicates the band corresponding to the full-size EF-G and the gray arrow points to the truncated product generated due to TEL-induced translation arrest at the codon 358 of the *fusA* gene (5).

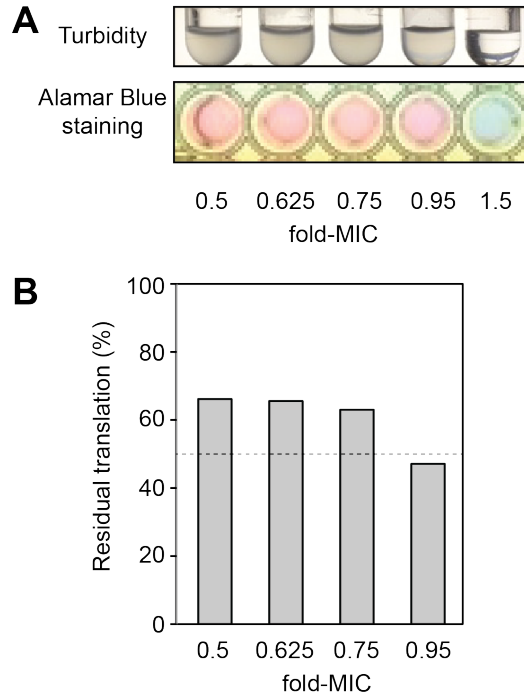


Figure S3. Reducing of the general translation rate by two-fold does not prevent cell growth and proliferation. (A): At near-MIC concentrations of the protein synthesis inhibitor chloramphenicol, translation rate in *E. coli* cells (strain BWDK) decreases approximately two-fold (dashed line marks a 50% decrease in the translation rate). Nevertheless, cells synthesizing all proteins at approximately 50% level continue to grow and multiply (B). In (B) cells were diluted to the final optical density of $A_{600} = 0.025$ in the same defined medium that was used for measuring translation rate (see Materials and Methods) and then grown overnight at 37°C in 15 ml tubes. Aliquots of the overnight cultures were placed into a 96-well plate and stained with Alamar Blue (blue color – no cell growth, pink color – live cells).